Accepted in Freshwater Science: Volume 40 March 2021

Contrasting Raz–Rru stream metabolism and nutrient uptake downstream of urban wastewater effluent sites

Sarah H. Ledford[1,4], Marie Kurz[2,5], and Laura Toran[3,6]

[1]Department of Geosciences, Georgia State University, 730 Langdale Hall, 38 Peachtree Center Avenue, Atlanta, Georgia 30303 USA

[2]Academy of Natural Sciences of Drexel University, 1900 Benjamin Franklin Parkway, Philadelphia, Pennsylvania 19103 USA

[3]Department of Earth and Environmental Science, Temple University, 1901 N 13th Street, Philadelphia, Pennsylvania 19122 USA

E-mail addresses: [4]sledford@gsu.edu; [5]marie.kurz@drexel.edu; [6]ltoran@temple.edu

Received 06 January 2020; Accepted 08 September 2020; Published online _____

Abstract: Understanding how key stream-ecosystem functions respond to wastewater-treatment-plant effluent is critical for assessing the ability of stream ecosystems to ameliorate anthropogenic nutrient loading and to effectively manage and restore impacted systems. We evaluated in-stream metabolism, reactive solute transport, and nutrient uptake along two 1.5 to 2 km-long reaches of a 2nd-order stream in the urbanized suburbs of Philadelphia, Pennsylvania USA, each directly downstream of a wastewater treatment plant outfall. We compared resazurin–resorufin (Raz–Rru) based metabolism with nutrient uptake and dissolved oxygen (DO) metabolism calculations. Plateau co-injections of the Raz–Rru metabolic tracer system and fluorescein provided integrated stream-metabolism measurement. We sampled tracer concentrations hourly along longitudinal profiles and recorded them continuously, along with DO, at 2 discrete locations. The smaller reach 1, characterized by higher nutrient concentrations and canopy cover, had higher short-term transient storage and Raz uptake velocity. In contrast, reach 2, with lower nutrient concentrations and less canopy cover, had higher nitrate and phosphorus uptake along with higher rates of gross primary productivity (GPP) and ecosystem respiration (ER). Temporal analysis indicated nitrate uptake increased over the afternoon at reach 2, whereas Raz uptake declined at both reaches. Our results suggest that nutrient uptake and GPP are sensitive to excessive nutrient concentrations and light in our system. In contrast, lower light and higher transient storage are likely driving larger, reach-scale spatial differences in Raz-based ER. Increasing nitrate uptake at reach 2, which lags behind diel DO concentrations, is likely the result of assimilatory N uptake coupled to GPP moderated by nitrification and denitrification, whereas decreasing rates of Raz transformation are likely related to diel variation in heterotrophic uptake. Our ability to resolve sub-daily changes in ER illustrates one of the key advantages of the Raz–Rru tracer system. However, our results also show the need for further

investigation into the drivers of sub-daily ecosystem metabolism in streams as well as the mechanistic differences between DO- and Raz-based estimates of ER. Contrasting results from different measures of metabolic activity between reaches and over time highlight the complexity of metabolic processes in high-nutrient systems.

Key words: in-stream metabolism, wastewater treatment plant, nutrient uptake, nitrate, total dissolved phosphorus, urban stream, resazurin

Anthropogenic inputs of nutrients to streams, including effluent from wastewater treatment plants (WWTPs), are a major driver of excessive nutrient loading and impaired water quality in streams worldwide. Increased inputs of nutrients to streams lead to increased algae growth, decreased dissolved oxygen (DO), and fish mortality (Dodds and Welch 2000, Smith 2003, Carey and Migliaccio 2009). In the United States (US), hypoxic zones in receiving waters continue to grow despite efforts throughout the country to curb nutrient inputs (van Meter et al. 2018). Although understanding the impacts of both point and non-point sources is required to fully quantify nutrient budgets, WWTPs are particularly important because they contribute to large nutrient loads in receiving streams. Despite improvements in treatment technology, US wastewater effluent that has gone through biological-nutrient-removal tertiary treatment typically still contains 3 to 8 mg/L of total nitrogen (TN) and 1 to 2 mg/L of total phosphorus (TP), and upgrading plants to further remove nutrients before discharge is cost-prohibitive (Carey and Migliaccio 2009). The fate of WWTP-derived nutrients in streams and their influence on stream-ecosystem function require further study.

The addition of nutrients and organic carbon, as well as changes in nutrient uptake rates, in WWTP-impacted streams can alter magnitude and patterns of ecosystem respiration (ER) and gross primary production (GPP). Gücker et al. (2006) found ER rates as high as –59 g O_2 m^{-2} d^{-1} downstream of WWTPs in German streams. Aristi et al. (2015) saw increases in ER downstream of WWTPs, whereas Wassenaar et al. (2010) found that the ER response downstream from WWTPs varied with season. GPP responses to effluent are more variable than ER, with observed rates as high as 59 g O_2 m^{-2} d^{-1} downstream of WWTPs (Gücker et al. 2006). This variation in response to effluent may be driven by changes in other environmental conditions besides nutrient concentrations, similar to what is seen in higher-nutrient urban streams without effluent. In those

cases, changes in riparian shading were an important driver in longitudinal GPP change (Ledford et al. 2017, Reisinger et al. 2019).

Although WWTP effluent increases nutrient concentrations in streams, the efficiency of nutrient uptake (i.e., concentration relative to flux) typically declines, driven by saturation kinetics (Dodds et al. 2002, Mulholland et al. 2008). Uptake lengths of N can increase downstream of WWTPs (i.e., less uptake), with some studies finding almost half of the studied streams showing no net nutrient retention (Martí et al. 2004, Gibson and Meyer 2007, Figueroa-Nieves et al. 2016). Another study found that nitrate uptake efficiencies did not have a uniform response to discharge and increased nutrient loads from 2 WWTPs (Gücker et al. 2006). Downstream of 1 plant, uptake rate and uptake velocity did not change, whereas the other plant showed large increases in both variables. Nutrients from WWTP effluent can be taken up via assimilatory and dissimilatory pathways. Assimilatory pathways result in the incorporation of nutrients into biomass, whereas dissimilatory pathways, including denitrification, include the use of nutrients as electron acceptors, changing the molecular form of the nutrient (Burgin and Hamilton 2007, Burgin et al. 2011).

Many metabolic processes, including assimilatory and dissimilatory uptake, vary with daily frequency, although the timing of these processes, and of resulting changes in stream solute concentrations, are not always predictable. For example, daytime autotrophic nitrate uptake, which is coupled to GPP, can lead to lower nitrate concentrations during the day relative to a nighttime peak. In contrast, assimilatory P uptake and denitrification do not have consistent diel cycles (Heffernan and Cohen 2010, Nimick et al. 2011 and references therein, Cohen et al. 2013), and we know very little about diel variations in heterotrophic activity or uptake. Resolving diel signals and process dynamics in streams receiving WWTP effluent is further

confounded by the co-occurrence of diel shifts in effluent quantity and quality and diel variations in nutrient demand and uptake (Gammons et al. 2011). Rahm et al. (2016) measured rapid uptake of nutrients downstream of a WWTP in central New York, USA, and although they could not determine the pathway, molecular assays indicated that denitrifying communities were being released in the effluent. The molecular form of N in the effluent understandably plays a large role in its fate.

Understanding how ecosystem functioning responds to WWTP effluent inputs (enhanced or inhibited) and what controls spatial and temporal variability in response (nutrient loading, effluent magnitude, hydrologic variability, metabolically active transient storage) is critical to assessing the capacity of stream ecosystems to ameliorate anthropogenic nutrient loading. These processes are all theoretically linked, and previous studies have compared stream metabolism (DO- or resazurin-resorufin [Raz-Rru]-based) and nutrient cycling in WWTP-impacted systems (ex. Gücker and Pusch 2006, Aristi et al. 2015, Ribot et al. 2019) and DO-based stream metabolism and Raz transformation (ex. González-Pinzón et al. 2012, 2014, 2016, Kurz et al. 2017, Knapp and Cirpka 2018). Raz transformation rates have not been reported previously in a WWTP-impacted stream system although Raz has been applied to study the metabolic activity of WWTP-derived sludge (Strotmann et al. 1993; McNicholl et al., 2007) and the metabolic response of WWTP-impacted flume biofilms to labile carbon (Ribot et al. 2019). The complexity of metabolic processes in time and space suggests that applying methods that resolve different processes over different scales is important to unravelling the key drivers of coupled metabolic processes in WWTP-impacted systems. Our goals in this study were: 1) to compare metabolic processing of effluent inputs from 2 WWTPs on the same stream, 2) to assess if hourly variations in metabolic activity occur in response to nutrient or temperature variation over the course of an

afternoon (~5 h), and 3) to compare the results of 3 methods measuring rates of whole-stream metabolic processes (Raz–Rru transformation, uptake of nutrients, and DO-based GPP and ER).

We hypothesized that: 1) the reach with a higher portion of WWTP input (and higher nutrient concentrations) would have lower rates of metabolic activity because of nutrient saturation, 2) metabolic rates would increase through the afternoon as nutrient concentrations and temperature rose as part of a diurnal effluent cycle, and 3) spatial and temporal patterns in metabolic parameters, including nutrient uptake, aerobic respiration, and whole-stream ER and GPP, would vary consistently between reaches as measured through the 3 methods of metabolism evaluation (Raz–Rru transformation, nutrient uptake, and DO-based GPP and ER).

METHODS

Site description

Wissahickon Creek is a 3rd-order stream at its outlet with the Schyulkill River and flows through Montgomery and Philadelphia counties, Pennsylvania, USA (Fig. 1A). It is a 166 km^2 suburban-to-urban watershed with a population of 222,000 (Center for Sustainable Communities 2014). Four WWTPs are permitted to discharge into the stream: 2 on the main stem and 2 on Sandy Run Tributary (Fig. 1A). The stream is listed as impaired because of nutrients, nuisance algae, and sediments (United States Environmental Protection Agency 2003). Although 51% of the watershed has impervious or low-pervious land cover, the corridor along the Wissahickon has benefited from open space protection. About 75% of the upper watershed has a forested riparian buffer on 1 or both sides, with that number increasing to 80% for the entire watershed because of forest cover in Fairmont Park, Philadelphia (The Heritage Conservancy 2012).

This paper focuses on the upper half of the main stem of the creek where the uppermost 2 WWTPs discharge. We chose these 2 sites because they have differing percentage of flow coming from the WWTP, resulting in differing nutrient concentrations downstream of their respective outfalls. In the headwaters, Upper Gwynedd WWTP effluent, contributes ~70 to 80% of discharge during baseflow downstream of this plant (reach 1; Fig. 1B). Grab samples show the effluent typically has 20 to 30 mg N/L of nitrate and 0.25 to 0.35 mg total dissolved phosphorus (TDP)/L. Effluent discharge generally exhibits a daily pattern of a morning rise, daytime plateau, and overnight fall. Previous longitudinal grab samples showed a downstream decrease in nitrate for 10 km downstream of the plant but did not show much change in TDP concentration over the same distance, potentially indicating different processing controls for the 2 nutrients. Reach 1 is ~2 km in length, has an average wetted width of 8.4 m, and an average depth of 22 cm (Table 1). This width combined with mature trees in the riparian zone results in a mean riparian canopy cover of 65%, along this reach (Fig. S1A). Similar high nutrient loads and longitudinal changes in nutrients have been observed in the downstream reaches below 2 of the other WWTPs in the watershed (Ledford and Toran 2020). In contrast, neither nitrate nor phosphorus show a decrease in concentration downstream of Ambler WWTP, which is ~10 km downstream of the Upper Gwynedd WWTP (Fig 1C). The Ambler WWTP effluent contributes ~40 to 50% of the total baseflow downstream of the plant (reach 2). Effluent nutrient concentrations range from 15 to 25 mg N/L of nitrate and TDP concentrations are highly variable, ranging from 0.2 to 1.5 mg P/L. Effluent discharge typically peaks in the morning and evening, with falling discharge during the early afternoon and overnight. Reach 2 is ~1.5 km in length with an average width of 19 m, more than twice the average width of reach 1. Its average depth of 21 cm is similar to that of reach 1 (Table 1). Reach 2's wider channel leads to a mean 55% canopy cover (Fig. S1B).

Experimental design

To measure the impact of WWTP effluent on stream ecosystem function, we used 3 independent measures of whole-stream metabolic processing at various spatial and temporal resolutions in the 2 study reaches. First, we used plateau injections of the reactive tracer Raz and calculated longitudinal estimates of aerobic respiration and the relative influence of metabolically active transient storage to whole-stream metabolism at sub-daily timescales. Raz undergoes an irreversible transformation to Rru under the mildly reducing conditions produced by respiring cells (O'Brien et al. 2000, Haggerty et al. 2008, Knapp et al. 2018). Thus, the rate of Raz–Rru transformation represents an integrated measure of (near-instantaneous) whole-system aerobic ecosystem respiration. The Raz–Rru system has been used broadly to assess the reactivity of stream reaches and to identify the portion of transient storage that is metabolically active (Argerich et al. 2011, González-Pinzón et al. 2012, 2014, Blaen et al. 2018, Ward et al. 2019). Second, we calculated nitrate and TDP retention downstream of the WWTP inputs at sub-daily timescales based on the longitudinal declines in concentration (Martí et al. 2004). Third, we calculated daily rates of whole-stream gross primary productivity (GPP) and ecosystem respiration (ER) at the midpoint of each study reach using the 1-station diel dissolved oxygen (DO) method (Hall and Hotchkiss 2017).

Stream solute tracer injections

Tracer injections To calculate reach and sub-reach scale transient storage and aerobic respiration we used plateau injection tests of conservative and metabolically reactive tracers combined with the nitrate and TDP inputs from the WWTP effluent (Martí et al. 2004). We

conducted an in-stream constant-rate injection of the conservative tracer fluorescein and reactive tracer Raz downstream of both WWTP effluent input points targeting a 4 to 5 h daytime plateau of ~30 ppb fluorescein and ~50 ppb Raz. At reach 1, we mixed 400 g fluorescein and 646 g Raz powder with 100 L of tap water in an opaque mixing drum and injected across the stream width 94 m downstream of the WWTP input at a rate of 2.7 to 2.8 mL/s for ~9.5 h (4:36–~14:06, 26 September 2017; Fig. 1B). Similarly, at reach 2, we mixed 400 g fluorescein and 626 g Raz powder with 100 L of tap water in an opaque mixing drum and injected across the stream width 150 m downstream of the WWTP input at a rate of 3.1 mL/s for a duration of 8:33 hours (7:43–16:16, 12 September 2017; Fig. 1C). We measured the injection flow rate into the stream periodically throughout both injections to account for potential variation, which was negligible.

Tracer concentrations were evaluated with both grab samples and data logging sensors. We measured concentration breakthrough curves (BTC) of fluorescein, Raz, and Rru at 10-s resolution with 2 calibrated in-situ GGUN FL30 fluorometers (Albillia Co., Neuchâtel, Switzerland; Lemke et al. 2014) located at 1494 m and 2894 m downstream of the reach 1 effluent input and 650 m and 1250 m downstream of the reach 2 effluent input (Fig. 1B, C). A 3rd fluorometer measured only fluorescein at 694 m and 1750 m in reaches 1 and 2, respectively. We collected longitudinal grab samples for analysis of major anions, cations, nutrients, and the concentrations of fluorescein, Raz, and Rru at hourly resolution during the tracer plateau. We collected hourly samples from 12:15 to 16:15 (with a final sample at 17:00) at reach 1 every 200 m along the study reach from 494 m downstream of the effluent input (400 m downstream of the injection point) to 2094 m downstream. We collected hourly samples from 12:30 to 16:30 at reach 2 every 100 m along the study reach from 550 m downstream of the effluent input (400 m downstream of the tracer injection point) to 1650 m downstream. There are differences in

longitudinal spacing because the number of sample sites was the same at both tests but the two reaches had different distances to the nearest major hydrologic feature (a low-head dam at reach 1 and a tributary at reach 2). We collected additional grab samples at the fluorometer locations pre- and post-plateau for analysis of tracer concentrations to cross-check the calibrated fluorometer BTC concentrations. We field filtered all Raz, Rru, and fluorescein grab samples through a 0.22-µm-glass-fiber filter and stored them at 4°C in amber glass vials until analysis. Within 48 h of collection, we analyzed samples on a PTI Quantamaster™ QM-4-CW lab spectrofluorometer (Photon Technology International Inc., Birmingham, New Jersey, USA). We created manual calibration curves at 490 nm excitation and 503 nm emission for fluorescein (Siejak and Frackowiak 2005), 570 nm excitation and 573 nm emission for resorufin, and 602 nm excitation and 621 nm emission for resazurin (Haggarty et al. 2008). We selected excitation peaks from literature values and chose emission peaks by selecting the peak emission from scans of standards of each dye run at the peak excitation wavelength reported in the literature.

Transient storage metrics Transfer functions are representative of subreach travel time distribution and reflect both in-stream and hyporheic transport and associated advective, dispersive, and short-term storage processes. To determine transfer functions for the subreaches between fluorometers, we used the nonparametric deconvolution approach described in Cirpka et al. (2007), and the associated MATLAB® (The MathWorks®, Inc., Natick, Massachusetts) code, to analyze injection input signal and conservative tracer BTCs. To characterize and compare this transport and storage behavior between study reaches, we calculated a series of transport and transient storage metrics for each subreach transfer function, following the equations in Ward et al. (2016), Schmadel et al. (2016), and Ward et al. (2019). Metrics included the 1st temporal

moment, M_1 (h), representing the mean travel time, the 2nd central temporal moment, μ_2 (h^2), representing the temporal variance or symmetrical spreading, the 3rd central temporal moment, μ_3 (h^3), representing the temporal extent of late-time tailing, the coefficient of variation, CV, representing symmetrical spreading relative to travel time, skewness, ɣ, representing asymmetrical late-time tailing, and apparent dispersion, D_{app} (m^2/h). Advective travel time, t_{ad} (h), was calculated as the peak time of the transfer function. CV, skewness, and D_{app} all represent metrics normalized by the advective timescales, which serves to remove the variation in the transfer function caused by advection, thereby accounting for the influence of different advective timescales (due to reach length and discharge) on solute tracer responses.

Reach characterization We characterized stream reaches through field measurements and calculations of hydrologic properties. We recorded temperature and pH every 15-min during all grab sampling windows using a calibrated Pro Plus multiparameter meter (YSI™ Inc., Yellow Springs, Ohio) located at 1494 m and 550 m downstream of the effluent input in reach 1 and 2, respectively. At reach 1 we used HOBO® U20 (Onset® Computer Corporation, Bourne, Massachusetts) loggers to measure temperature and depth in the WWTP effluent input (0 m) and in-stream at 1494 m and 2194 m, and we used a YSI EXO²™ sonde to measure specific conductivity at 1494 m, all at 15-minute intervals. At reach 2, we used HOBO U20 loggers to measure temperature and depth below the effluent input (0 m), and at 650 m, 1200 m, and 1700 m. We measured specific conductivity at reach 2 with a HOBO U24 immediately below the effluent input at 0 m, a YSI EXO² sonde at 650 m, and a YSI 600 sonde at 1700 m, all measuring at 15-minute intervals. These logger records at both reaches are part of a larger spatial and temporal dataset of depth and specific conductivity within the Creek; 24-hours of data are

reported here for each site. We used a FlowTracker2® Handheld-ADV® (SonTek™, San Diego, California) to measure stream discharge during the grab sample collection windows at 2 locations in each reach, which we averaged. We used contemporary satellite imagery of the field site (GoogleEarth; Google, San Francisco, California) to estimate wetted area (m^2) and center-channel stream length (m), and we calculated stream width (m) as wetted area divided by length. We calculated specific discharge (m^2/s) as discharge divided by average reach width. We also used GoogleEarth imagery to estimate canopy cover (%), and we used a Welch's *t*-test with unequal variance to compare canopy coverage between the reaches. We calculated velocity (m/s) for each sub-reach between sampling points as the sub-reach advective travel time estimated from the BTCs divided by sub-reach length; we used these sub-reach velocities to calculate the length-weighted mean velocity of the two study reaches. We calculated stream depth (m) for each sub-reach as volume divided by wetted area, where volume is the product of discharge (see below) and the advective travel time; we again used these sub-reach depths to calculate the length-weighted mean stream depth of the two study reaches.

Raz–Rru transformation rates To estimate Raz–Rru transformation rates, we used the longitudinal profiles of Raz and Rru tracer concentrations from the grab samples collected during the tracer plateau, as in Kurz et al. (2017), using the analytical solution:

$$k_{t,ad} = [\ln(C_{Rru}/C_{Raz} + P) - \ln(C_{Rru,0}/C_{Raz,0} + P)]t_{ad}^{-1}$$

where $k_{t,ad}$ (/h) is the apparent Raz–Rru transformation rate coefficient, assuming transformation is a 1st-order process (Haggerty et al. 2008), C_{Rru} and C_{Raz} are the concentrations of Rru and Raz (ppb), $C_{Rru,0}$ and $C_{Raz,0}$ are the input concentrations of Rru and Raz, P is the production–decay ratio (unitless), and t_{ad} is the advective travel time (h), such that $k_{t,ad}$ is the slope of the regression

between travel time and the Rru:Raz ratio. By utilizing the Rru:Raz ratio in our calculations we eliminate the need to correct for conservative mass loss or dilution. We assume irreversible sorption of both tracers is minimal given the pH remained above 7.7 at both sites (Table 1) and that any mass losses of Raz or Rru other than the decay of Raz to Rru are minimal or equal between the 2 tracers; therefore, $P = 1$. The concentration of Rru at the injection site is theoretically 0, however, when solving for $k_{t,ad}$ as the slope of $\ln(C_{Rru}/C_{Raz} + 1)$ and t_{ad}, we do not enforce an intercept of 0. We interpolated the advective travel time to each sampling station from the downstream distance of each sampling site and the between-fluorometer sub-reach travel times calculated from the fluorometer BTCs. We used the fitlm function in MATLAB to test the slope of each sampling-period regression. $k_{t,ad}$ is reported as 0 for sampling periods with a *p*-value above 0.06 (Table S1).

Raz to Rru transformation rates have been shown to be proportional to changes in oxygen, which is a common measurement of respiration rates (González-Pinzón et al. 2012). Therefore, estimated $k_{t,ad}$ can be used as a proxy of instantaneous rates of ecosystem respiration. To compare Raz transformation values among reaches with different hydrologic conditions, we used the uptake velocity of Raz ($v_{f\text{-}Raz}$, mm/min), calculated as

$$v_{f\text{-}Raz} = k_{t,ad}\, d$$

where d (m) is the average water depth. $v_{f\text{-}Raz}$ can be thought of as the effective velocity of the transformation of Raz into Rru (Haggerty et al., 2014). We used the fitlm function in MATLAB to test temporal trends in all Raz transformations. To compare Raz transformation between sites, when there was strong evidence of uptake, we used the ttest2 function in MATLAB to perform a Welch's *t*-test with unequal variance.

Nutrient uptake

For our 2nd whole-stream metabolism method of calculating nitrate and TDP retention downstream of WWTP inputs, we analyzed the longitudinal grab samples for these nutrients. We field filtered 60-mL samples for nitrate and chloride to 0.22 μm and froze them until analysis. We measured nitrate and chloride, along with other anions, on an ICS-1000 ion chromatography system (Dionex™ Sunnyvale, California). We collected 125 mL of sample in pre-cleaned bottles for total dissolved phosphorus (TDP), field filtered samples to 0.22 μm, and acidified them with 3 drops of trace-metal-grade nitric acid. We stored samples at 4°C until analysis on an iCAP™ 7000 ICP-OES system (Thermo Scientific™, Waltham, Massachusetts) for TDP and other cations. Following methods of Martí et al (2004), we treated the WWTP effluent as a nutrient injection, with nitrate and TDP concentrations normalized to chloride at each sampling location and then used to calculate uptake parameters. We calculated uptake (k) as the negative slope of the regression between advective travel time (t_{ad}) from the effluent input and the natural log of dilution-corrected nutrients. Linear regressions fit these relationships best, indicating pseudo-1st-order decay (Hensley et al. 2014), and we used the fitlm function in MATLAB to test the slopes of these regressions (Table S1). We consider k to be detectible when the slope of the regression had a p-value <0.06. Choosing this alpha level allowed us to include 2 sampling periods at reach 1 with k that appeared likely important even though not as strongly detected as other sampling periods. Time periods that did not have detectible uptake or showed nutrient release are reported as 0.

For the time periods with detectible k, we calculated uptake velocity, uptake length, and areal uptake rates. Uptake velocity (or mass transfer coefficient) takes into account differences in

stream velocity, resulting in the rate of movement from the stream to the bed. We calculated uptake velocity (v_f) as:

$$v_f = kd.$$

Nutrient uptake length is conceptualized as the average distance a nutrient molecule travels downstream in inorganic form before being assimilated. We calculated uptake length (S_w) as:

$$S_w = Q/(v_f w),$$

where Q is mean stream discharge in m^3/s and w is mean wetted width in m. Finally, the areal uptake rate takes into account different levels of ambient nutrient concentrations, resulting in the mass assimilated per area streambed per unit time (Stream Solute Workshop 1990). Areal uptake rate (U) was calculated as:

$$U = v_f concentration,$$

where *concentration* is the mean nutrient concentration of the reach during each sampling time (Stream Solute Workshop 1990). We identified temporal trends in nutrient uptake in the same manner as Raz by using the fitlm function in MATLAB. When there was positive, non-zero uptake, we compared uptake parameters (k, v_f, and U) between the reaches with a Welch's t-test with unequal variance (ttest2 function in MATLAB).

Daily whole-stream metabolism

To obtain our 3rd measure of whole-stream metabolic processing, we used the 1-station diel DO method (Hall and Hotchkiss 2017). We used in-situ sensors (YSI EXO^2 multiparameter sonde and Onset HOBO U20 and Pendant loggers) to measure DO, temperature, water depth, and light every 15-minutes at the midpoint of the 2 study reaches: 1494 m downstream of the effluent input at reach 1 (Fig. 1B) and 650 m downstream of the effluent input at reach 2 (Fig.

1C). These records are part of a larger spatial and temporal dataset of DO measurements within the Creek; approximately 7 to 8 days of data are used here, from 22–29 September 2017 for reach 1 and 12–18 September 2017 for reach 2. Solar noon varied from 12:57 EDT on 12 September to 12:51 EDT on 29 September 2017. We used the *StreamMetabolizer* package (Appling et al. 2018) in R (version 3.6.1; R Project for Statistical Computing, Vienna, Austria) to calculate daily estimates of whole-stream GPP, ER, and net ecosystem production (NEP). We used the Bayesian approach and did not pool K600 values, with K600 values calculated by the model for this period as 2.8 ± 0.5/d at reach 1 and 5.1 ± 1.2/d at reach 2. R^2 for the fit between modeled and observed DO for these time periods averaged 92% at reach 1 and 99% for reach 2. We did a Welch's *t*-test with unequal variance to compare GPP and ER over the period modeled to test for differences.

RESULTS

Stream solute tracer injections

Solute transport Transient storage, one driver of metabolism rates, showed different storage processing between reaches. We observed lower discharge and longer advective travel times in reach 1 relative to reach 2 (Table 1). Both central moments were higher in reach 1, consistent with the longer reach 1 advective transport timescales that allowed time for non-advective processes, including dispersion and transient storage, to act on the tracer signal. The CV, skewness, and D_{app} metrics, all normalized by this advective time scale, provide a more accurate comparison of transient storage between study reaches. CV was similar across both reaches, whereas D_{app} and skewness were higher in reach 1. This result indicates that both dispersion and

short-term storage processes were higher in reach 1 relative to reach 2 even when accounting for the longer advective timescales in reach 1.

Reach characterization Discharge during the tests averaged 0.09 m^3/s at reach 1 and 0.34 m^3/s at reach 2 (Table 1). Depths recorded by loggers indicate minimal change in discharge over the course of sampling, with <1 mm of change at reach 1 sites and 1 to 2 cm of change at reach 2 sites (Fig. 2B, F). Temperature increased ~1.8 to 1.9°C over the sampling period in reach 1 and ~0.6 to 1.8°C in reach 2 (Fig. 2A, E). 1 location was monitored for specific conductivity in reach 1, showing a plateau at the beginning of sampling followed by an increase over the afternoon (Fig 2C). Specific conductivity increased over the afternoon at the reach 2 WWTP, but this change was attenuated with distance (Fig. 2G). Canopy coverage at reach 1 averaged 35.3% open channel, and reach 2 had more open channel (44.8%; $p = 0.01$, df = 19.4; Fig. S1).

Raz-based metabolism All sampling times at reach 1, and 4 of 6 sampling times at reach 2, showed detectible transformation of Raz to Rru (all tests of regressions $p < 0.06$ except 16:15 and 17:00 at reach 2; Table S1). Cumulative Raz transformation to Rru increased with longitudinal distance in both study reaches (Fig. S2). The intercept of this relationship suggests an initial concentration of 10% Rru in the injection, which is consistent with the purity of Raz injected. Estimates of retardation factors from our tests are 1.08 for Rru and 0 for Raz, lower than those reported in Lemke et al. (2014; 1.36 and 1.22, respectively; Fig. S3). These low retardation factors indicate there was negligible sorption of Raz and Rru at both sites, consistent with the high pH values at the sites (Table 1). Raz to Rru transformation rates, $k_{t,ad}$, and the uptake velocity of Raz, $v_{f\text{-}Raz}$, varied by an order of magnitude between the 2 study reaches

(Table 2), with higher uptake velocities being observed in reach 1 than reach 2 (p = 3.5E–4, df = 4.4; Fig. 3). In both reaches, $k_{t,ad}$ and $v_{f\text{-}Raz}$ declined over the course of the afternoon observation period, $v_{f\text{-}Raz}$ from 0.13 to 0.08 mm/min (–33%; p = 0.02, df = 3, Fig. 3) in reach 1 and from 0.02 mm/min to below detection in reach 2 (p = 0.007, df = 4, Fig. 3).

Nutrient uptake

Our 2nd method of ecosystem metabolism evaluation, measuring nutrient retention downstream of WWTPs, showed differences between reaches. Nitrate concentrations in reach 1 were nearly twice as high as those in reach 2 (p = 4.1E–9, df = 7.5); however, nitrate fluxes in reach 1 were <half the fluxes measured reach 2 (Table 2). Concentrations from each individual grab sample site generally increased over the afternoon, although mean concentration across the entire reach during the test period only increased at reach 2 (p = 0.03, df = 4; Table 2). Nitrate concentrations decreased with distance downstream of the plant at both sites during most sampling periods. At reach 1, all samplings showed detectible uptake, and at reach 2, 3 time periods had detectible uptake of N (15:15, 16:15, and 17:00), 1 had marginal uptake (14:15), and 2 had negative uptake (12:15 and 13:15; Table S1, Fig. S4A, C). Nitrate uptake length at reach 1 ranged from 7.9 to 16.9 km, whereas reach 2 had late-afternoon (15:15, 16:15, and 17:00) uptake with lengths from 6.7 to 9.0 km (Table 2). In addition, areal rates of NO_3^- uptake showed indications of saturation kinetics, with very high areal uptake rates (988–2554 mg N m^{-2} d^{-1}) but low uptake velocities (0.038–0.160 mm/min) between sites at both reaches during periods with uptake. When considering only sample periods with detectible positive uptake, uptake velocities were lower in reach 1 than reach 2 (p = 0.02, df = 2.3), as was areal uptake (p = 0.03, df = 2.8). There was no measurable change in nitrate uptake rates over the afternoon at reach 1, whereas

both v_f (p = 0.009, df = 4; Fig. 3) and U (p = 0.005, df = 4) increased over the afternoon at reach 2.

Phosphorus concentrations and trends also differed between the 2 reaches. TDP concentrations were approximately 20% higher in reach 1 than 2 (p = 3.6E–4, df = 5.8; Table 2). TDP increased over the afternoon at all sites in reach 1, but was more variable at reach 2, plateauing at many sites in the later afternoon. Average whole-reach TDP concentrations increased over the afternoon at both reaches (reach 1: p = 0.002, df = 4; reach 2: p = 0.04, df = 5; Table 2). Over reach 1, 3 time periods had detectible uptake for TDP (14:30, 15:30, and 16:30; Table S1), 1 time period showed marginal uptake (13:30), and 1 time period had a negative uptake (12:30). At reach 2, only 1 time period had detectible uptake for TDP at reach 2 (12:15), 2 time periods were marginal (13:15 and 17:00), and the remaining 3 time periods had negative uptake (14:15–16:15; Table S1, Fig. S4B, D). Neither reach had a temporal trend in TDP uptake. Because of the small number of samples with detectible uptake, spatial statistics for TDP could not be calculated.

DO-based metabolism

The 3rd method of metabolism evaluation, the 1-station diel DO method, also showed differences between the 2 reaches. On the day of the injection, DO varied from 1.86 mg/L to 9.59 mg/L at reach 1, with the minimum at 5:45 and the peak at 16:45 (Fig. 2D), and temperature ranged from 22 to 26°C (Fig. 2A). At reach 2, DO ranged from 7.44 mg/L to 12.10 mg/L, with the minimum at 0:45 and maximum at 11:30 (Fig. 2H), and temperature ranged from 16 to 20°C (Fig. 2E). Using 8 d of DO measurements, both sites were always net heterotrophic, although reach 1 was more heterotrophic (i.e., had more negative NEP). At reach 1, mean GPP was 2.7 g

O_2 m^{-2} d^{-1} (± 1.6 SD), and mean ER was –7.4 g O_2 m^{-2} d^{-1} (± 1.1). In contrast, mean GPP at reach 2 was 7.0 g O_2 m^{-2} d^{-1} (± 2.2), and mean ER was –10.1 g O_2 m^{-2} d^{-1} (± 2.3). In-stream productivity was higher in reach 2 than reach 1 (GPP: $p = 0.002$, df = 10.9; ER: $p = 0.022$, df = 8.2, Fig. S5).

DISCUSSION

This study examined spatial and temporal patterns of three different metabolic indicators downstream of two wastewater treatment plants, reporting results from the Raz-Rru tracer system in a WWTP-impacted system for the first time. One of the key advantages of the Raz–Rru tracer system over traditional DO-based daily estimates is the ability to resolve sub-daily changes in ER and provide daytime heterotrophic metabolism estimates. The Raz-Rru tracer confirmed low metabolic activity, potentially due to nutrient saturation, along with low DO-based GPP and ER rates. Spatial differences were observed downstream from two WWTPs only 10 km apart, but apparently not related to their differing effluent contributions as expected. Furthermore, temporal variations were not consistent between the reaches or between the different metabolic indicators. In this section we discuss the drivers for these different responses and illustrate the need for multiple indicators to investigate ecosystem metabolism in streams.

Wastewater impacts on metabolic activity

Previous research has shown that downstream of WWTPs, effluent inputs saturate nutrient demand and reduce nutrient removal efficacy (Martí et al. 2004, Covino et al. 2010, Hensley et al. 2014), with concurrent effects on ER and GPP (Gücker et al. 2006), which our results support. Our observed rates for DO-based GPP and ER and nutrient uptake all fell within

the ranges seen at other WWTP-impacted sites, and other studies that used DO to measure productivity rates in WWTP-impacted streams reported rates that were both similar to ours (Aristi et al. 2015) and higher (Gücker et al. 2006). Along with similar GPP and ER rates, long uptake lengths have been measured for nitrate in most WWTP-impacted systems (Haggard et al. 2001, Martí et al. 2004, Gücker et al. 2006; Fig. 4), and our system showed the same pattern. Our high nitrate uptake rates were driven by extremely high nitrate concentrations in our streams, as expected downstream of WWTPs. Nitrate uptake velocities were low in our system, as seen in other eutrophic streams (Ensign and Doyle 2006, Gücker and Pusch 2006, Hall et al. 2009, Hensley et al. 2014). Low uptake velocities combined with long uptake lengths indicate that demand for nitrate was lower than the load. Phosphorus uptake was also on-par with other WWTP removal results (Martí et al. 2004, Haggard et al. 2001, Gücker and Pusch 2006). Gücker and Pusch (2006), Gücker et al. (2006), and Haggard et al. (2005) all reported a large range in TDP areal uptake rate, from approximately 14 mg P m^{-2} d^{-1} up to 2506 mg P m^{-2} d^{-1}, with many higher than the maximum of 80 mg P m^{-2} d^{-1} measured across our reaches. We infer that high nitrate and TDP concentrations do not limit rates of metabolic processing.

Raz transformation rates in a WWTP-impacted stream system have not been reported previously, but our Raz results are consistent with DO-based studies reporting reduced ER in such systems. The observed rates of Raz transformation are on the low end of values previously reported for natural and artificial stream systems not affected by WWTP. When compared with streams of similar size, the higher values observed in reach 1 are within the low end of the range of other reported values (Blaen et al. 2018, Knapp and Cirpka 2018) whereas those in reach 2 are an order of magnitude lower than previously observed values. These low Raz transformation

rates illustrate the sensitivity of the method, showing distinctly different rates in nearby WWTPs; the low rates also confirm the impact of nutrient saturation.

Drivers of spatial patterns in metabolic processes

Metabolic activity clearly differed between the 2 study reaches; however, this spatial difference was not consistent amongst the various metabolic metrics measured. Nitrate uptake rates and DO-based GPP and ER were all lower in reach 1, which had higher nutrient concentrations than reach 2, in support of our hypothesis 1. Reach 2 may also be less effective at P retention, given that more sampling times had no detectible P retention. In contrast, Raz transformation was higher in reach 1. This difference suggests that, counter to our hypothesis 3 and that proposed by Haggerty et al. (2009), the primary drivers of the spatial patterns in these metabolic processes were decoupled in our system.

Variable environmental conditions between reaches may have influenced nutrient dynamics and metabolism in our study. The corresponding differences in nutrient uptake and DO-based metabolism between reaches, and their inverse relationships with nutrient concentrations and canopy cover, suggest that excessive nutrient concentrations, shading, or both, inhibit both nutrient uptake and GPP and ER at reach 1 relative to reach 2. Such clear coupling between in-stream metabolism and nutrient uptake velocities is well supported in the literature (Heffernan and Cohen 2010, Hensley and Cohen 2016). The fact that our GPP rates are similar to urban streams with lower nutrient loads (Clapcott et al. 2016, Alberts et al. 2017) indicates that reduced light, more than excessive nutrients, may limit GPP in reach 1 (Bernhardt et al. 2018, Reisinger et al. 2019). Although both reaches have a similar depth, reach 2 is twice as wide as reach 1 (Table 1) with a more open canopy (Fig. S1), suggesting similar light

penetration to the benthic surface at both reaches but a greater and more highly lit surface area for benthic microalgae growth in reach 2. These differences indicates that photoautotrophic productivity and nutrient uptake may be more important than heterotrophic and dissimilatory activity in reach 2 relative to reach 1, at least in the afternoon. The relative predominance of photoautotrophic activity in reach 2 is also consistent with its lower relative transient storage (Table 1), potentially limiting the transport of nutrients from the water column to the subsurface and, thus, limiting denitrification. The spatial differences in nutrient uptake lengths between sites are inversely related to differences in specific discharge, which is the opposite of the scaling trend typically observed in streams (Hall et al. 2013). This inverse trend suggests that local reach conditions, including site-specific differences in nutrient uptake and GPP driven by light availability, nutrient concentrations, and benthic contact, rather than stream discharge, are the predominant drivers of the observed spatial differences in nutrient uptake.

Higher Raz transformation rates and uptake velocities were observed in reach 1 than reach 2. The higher rates were associated with higher nutrient concentrations (Table 2), dispersion (D_{app}), and short-term storage processes (skewness), as well as lower relative stream size (as measured by discharge and specific discharge) and light availability (as proxied by canopy coverage; Table 1). Unlike nutrient uptake, the higher nutrient concentrations in reach 1 do not appear to inhibit relative Raz transformation and, in fact, there is some evidence that higher nutrient concentrations can stimulate microbial respiration, at least in lower-nutrient systems (e.g., Ramírez et al. 2003, Halvorson et al. 2016). Thus, the higher Raz transformation rates in reach 1 are most likely the result of enhanced short-term transient storage processes, including hyporheic exchange, in-channel storage, or both, promoting higher heterotrophic

activity relative to reach 2. Reduced light availability and higher nutrient concentrations in reach 1 result in lower relative photoautotrophic activity relative to reach 2.

Drivers of temporal patterns in metabolic processes

Temporal differences in environmental conditions, and not WWTP effluent magnitude, appear to be driving differences between the reaches. Nutrient concentrations, nitrate uptake, water temperature, and Raz transformation rates were all observed to change over the course of the afternoon tracer tests (~12:00–17:00) in 1 or both study reaches. Although we did not directly measure light across the entire reaches, it presumably also changed (solar noon was at 12:54 ± 0:03). In contrast, neither the magnitude of WWTP effluent inputs nor stream discharge (as approximated by stream depth, Fig. 2B, F) showed a temporal change over the sampling period as we had expected.

The presence of temporal patterns in nutrient concentrations and uptake differed between the 2 reaches. Neither nutrient removal efficiency nor nitrate concentrations changed over the afternoon in reach 1, contrary to our hypothesis 2 that these parameters would be time varying along with effluent magnitude, although TDP concentrations increased. However, at reach 2, nitrate uptake, along with both nitrate and TDP concentrations, increased over the afternoon (Fig. 3). Although this reach 2 trend was in line with our hypothesis 2 and paralleled the temporal trend in temperature, it was not perfectly in-phase with rates of instantaneous GPP, which would be expected to mirror the reach 2 afternoon plateau in DO concentration (Fig. 2H). This offset in phase suggests that assimilation, which is typically tightly coupled to the timing of GPP (Heffernan and Cohen 2010, Kurz et al. 2013) was not the sole driver of the increasing rates of nitrate removal observed in reach 2. Higher daytime nitrification, enhanced by light, DO, and

temperature, has been shown to promote denitrification (Laursen and Seitzinger 2004), which could have been the case in this study. However, unlike many other WWTP-impacted systems (Martí et al. 2004, Figueroa-Nieves et al. 2016), ammonia concentrations are reasonably low in our WWTP effluent (<0.1 mg/L as reported by WWTPs), and nitrification of effluent is not likely to be a major factor influencing N cycling in our system. Further, unlike for other well-lit systems, our observations do not support inhibition of daytime denitrification in the subsurface by benthic microalgae productivity (Nimick et al. 2011 and references therein). The lack of other temporal trends in nutrient uptake highlights the complexity of disentangling diel nutrient processing dynamics, especially given the short length of our observation window. In addition, the time-varying response to nitrate and TDP uptake indicates complex interactions between nutrient concentrations, loads, and the timing of N and P demand by microbes (Heffernan and Cohen 2010, Cohen et al. 2013). We did not expect the variation in temporal change of nutrient uptake between reaches (including the lack of temporal change in reach 1), and this variation indicates that nutrient uptake at these sites may be decoupled from other temporal factors, including nutrient concentration, discharge, and temperature, at the timescale sampled.

In contrast to nutrient uptake, the observed temporal declines in $k_{t,ad}$ and $v_{f,Raz}$ at both reaches over the afternoon (Fig. 3) illustrate the ability of the Raz–Rru tracer system to resolve sub-daily changes in reach-scale ER but are opposite in direction from our expectation (hypothesis 2). Although it is well known that autotrophic processes, including increased rates of daytime photoautotrophic nitrate uptake and nighttime autotrophic P uptake, can vary with sub-daily frequency (Heffernan and Cohen 2010, Nimick et al. 2011 and references therein, Cohen et al. 2013), comparatively little is known about diel variations in heterotrophic activity or uptake. ER in streams is often assumed to be either diurnally stable, as is the case for the diel-DO

method for estimating stream metabolism (Odum 1956, Owens 1974), or to increase predictably with temperature, such as in the van't Hoff-Arrhenius equation. Testing these assumptions, González-Pinzón et al. (2016) observed no significant differences between daytime and nighttime respiration rates estimated from Raz transformation. They suggested this lack of difference was likely because most stream respiration takes place in the hyporheic zone where diurnal fluctuations in stream temperature and light are considerably attenuated. In contrast, Tobias et al. (2007) and Hotchkiss and Hall (2014) found evidence using stable oxygen isotopes that daytime ER was higher than nighttime. However, their estimates were subject to uncertainty resulting from estimated parameters, which limited their ability to further interrogate potential drivers of this daytime increase.

Previous research has reported increased biochemical reaction rates with temperature, and corresponding spatial and temporal coupling between temperature and ER in streams (Sinsabaugh 1997, Perkins et al. 2012, Beaulieu et al. 2013, Hotchkiss and Hall 2014). However, in our system surface water temperatures increased over the afternoon (Fig. 2A, E), reflecting an inverse relationship with $k_{t,ad}$ and $v_{f\text{-}Raz}$. Even if Raz transformations primarily occur in the subsurface, the temperature there is also expected to increase some, even accounting for a potential lag between surface and subsurface patterns. Likewise, temporal variation in nutrient concentrations does not appear to influence temporal patterns in $k_{t,ad}$ and $v_{f\text{-}Raz}$. Both nitrate (reach 2 only) and TDP concentrations increased during the observation window, inverse with Raz transformation, but there is no evidence that nutrients were limiting in our system. Also, comparison of the 2 reaches does not appear to support nutrient-concentration-inhibition of Raz transformation.

Light is the major driver of GPP in streams, which was illustrated in our study by the lower shading and higher GPP rates in reach 2. In turn, daily estimates of ER are often, but not always, predicted by GPP (e.g., Beaulieu et al. 2013), in part because of the availability of new or more labile carbon to drive ER (e.g., Kaplan and Bott 1982, De Lange et al. 2003, Heffernan and Cohen 2010). Tobias et al. (2007) and Hotchkiss and Hall (2014), suggest this relationship between light and ecosystem metabolism could downscale to sub-daily linkages. Further, daytime increases in benthic algae productivity have also been shown to increase oxygen penetration in the subsurface (Nielsen et al. 1990, Lorenzen et al. 1998), which would expand the aerobic zone for subsurface Raz transformation during the day. Our observed pattern of decreasing $v_{f\text{-}Raz}$ over the afternoon does not appear to clearly support either of these light-driven mechanisms. However, we note that our ability to fully resolve the drivers of the observed temporal change in Raz transformation rates is confounded by the short (4–5 hour) observation window during our tracer tests and the timing of this window (~12:00–17:00) that roughly spanned the period between the solar peak and the lagged peak in DO. This decline in $v_{f\text{-}Raz}$ appears to be in-phase with the diel pattern of daily solar radiation (declining after ~12:54). However, the timing of most light-driven metabolic processes, including GPP and assimilatory nitrate removal, lag behind the solar peak (Heffernan and Cohen 2010) and would, therefore, still have been increasing during the afternoon observation window. For instance, this lag was seen in DO concentrations, especially in reach 1 (Fig. 2D). The differences in temporal responses of the metabolic indicators illustrates the need for further investigation into the drivers of ecosystem metabolism in streams.

Contrasting metabolic indicators

The 3 metabolic indicators, Raz-transformation, nutrient uptake, and DO-based GPP and ER, differed in the patterns between reaches. Unlike our expectations (hypothesis 3), the trend in Raz-transformation did not mirror nitrate uptake or ER. Conversely, spatial nitrate uptake patterns were similar to those of DO-based GPP and ER, all which had higher rates in reach 2. The patterns also differed over the afternoon, with a decrease in uptake velocity for Raz in both reaches, an increase in nitrate uptake at reach 2, and no change for all other nutrient uptake velocities.

The relationship between Raz-based and DO-based measurements of respiration is dependent on the assumptions of each method. A lack of relationship between Raz-based and DO-based estimates of ER have been reported before within stream systems (Kurz et al. 2017, Knapp and Cirpka 2018) even though Raz transformation has been shown to be well correlated with oxygen turnover both in batch experiments and broadly across stream systems (González-Pinzón et al. 2012, 2014, 2016, Knapp and Cirpka 2018). However, this apparent contradiction could be attributed to methodological differences and assumptions. Raz transformation rates measured during the observation window of a tracer test are not necessarily representative of the full 24-h integral of the diel DO method. In our case, however, this explanation is not sufficient to account for the spatial difference in diel DO- and Raz-based respiration measurements. That is, respiration would have had to have been extremely variable over time and, in the case of reach 2, unrealistically high during the un-sampled periods of the day. Additionally, there could be losses of Raz or Rru through processes other than the decay of Raz to Rru, which would only matter if the relative magnitude of Raz vs Rru loss varied over space or time or both. Sorption of both tracers was negligible, but both Raz and Rru are somewhat sensitive to photodecay, with the timescale of Rru photodecay being an order of magnitude faster than that of Raz (10s of h vs

100s of h, respectively; Haggerty et al. 2008). Although relative differences in Raz vs Rru photodecay cannot explain the directionality in observed temporal patterns, they could contribute to the spatial differences between the 2 sites. Enhanced photodecay in the more open canopy of reach 2 would reduce the apparent k_d values, but an unrealistic increase in photodecay of >20-fold would be needed to account for the entire spatial difference observed.

More plausibly, we attribute the difference in DO- and Raz-based ER results to a lack of understanding of the physical or biological processes that drive Raz transformation in stream systems. It is possible that the tracer-based approach does not sample the same physical compartments of the ecosystem as the diel DO method, despite both being metrics of whole-stream oxygen consumption. Only flowpaths falling within the time period of the tracer test are reflected in the tracer observations, although plateau injections such as ours more completely sample longer flowpaths than are sampled by slug injections. Likewise, the differing results between methods may reflect a lack of biological process understanding regarding Raz transformation specifically or ecosystem metabolism more broadly, including the roles of heterotrophs, autotrophs, or oxygen-cycling reactions. Notably, González-Pinzón et al. (2012) demonstrated that the magnitude of Raz transformation relative to oxygen loss differed between pure cell cultures, suggesting that microbial community structure could strongly affect the degree of Raz transformation observed relative to oxygen loss. This dependency likely holds for Raz transformation relative to other microbially-mediated functions, such as nutrient cycling.

The inverse spatial patterns observed in the uptake velocities of nutrients and Raz suggest the drivers of nitrate uptake and respiration are decoupled in our system. Although Haggerty et al. (2009) predicted Raz transformations and nutrient uptake rates could be correlated if transient storage and nutrient retention are related, our findings indicate the limitations of this assumption.

It is understood that metabolic processes, while coupled, are not always synchronous in their timing. For example, the timing of assimilation varies for different elements at different times of day because of biota processing along different pathways (Heffernan and Cohen 2010, Cohen et al. 2013, Appling and Heffernan 2014, Hensley and Cohen 2016, Bernhardt et al. 2018), and rates of denitrification have been shown to be driven by the previous day's GPP (Heffernan and Cohen 2010). Such lags could explain the observed temporal trend in sub-daily Raz transformation, but our limited observation window and differences in temporal trends in nutrient uptake (or lack thereof) limit our ability to resolve these nuances further.

Collectively, our results demonstrate that identifying the drivers of different measures of metabolic rates in systems with complex physical and chemical inputs, such as stressed urban streams, can be challenging. In addition, the 2 reaches, which are only 10 km apart, show large spatial and temporal differences in metabolic processing within each measurement method, highlighting the complexity of metabolic responses to small changes in hydrology, geomorphology, and light availability. The extremely high nutrient flux at both sites supports a system that is energy, not nutrient, limited (Reisinger et al. 2019). In the wider, more open-canopy and lower nutrient reach 2, photoautotrophic productivity and nutrient uptake appear to be more important than heterotrophic and dissimilatory removal. In contrast, heterotrophic activity appears to be more important in reach 1, where higher transient storage potentially facilitated the transport of nutrients from the water column to the subsurface. Temporal trends in nitrate uptake, only discerned in reach 2, could be the result of time-varying rates of primary productivity and coupled nitrification–denitrification.

Different observed outcomes among the multiple methods of metabolism evaluation suggests a measure of uncertainty should be incorporated into single-method stream metabolism

estimates in WWTP-impacted systems. The Raz-Rru tracer system provides a unique opportunity to advance our understanding of the drivers of heterotrophic activity, especially at sub-daily timescales. Combining and comparing multiple measures of metabolic activity allows for more complete inference of the factors driving temporal and spatial patterns in stream metabolic processes. Further research is needed to support a more mechanistic understanding of the drivers of Raz transformation relative to often contrasting DO-based estimates of ER and other metrics of ecosystem metabolism in streams.

ACKNOWLEDGEMENTS

Author contributions: SHL, MK, and LT developed the research question, organized and conducted the field work, and analyzed and interpreted the data. SHL conducted the lab work and dissolved oxygen modeling. MK did the Raz–Rru and transient storage modeling. SHL and MK wrote the manuscript with input from LT. All authors edited the manuscript.

Funding for this work was provided by the National Science Foundation grants EAR 1750453 and EAR 1752016 and by the William Penn Foundation grant 08-16 to Temple University. Sampling was made possible by students from Temple University along with community volunteers from the Wissahickon Valley Watershed Association and the Academy of Natural Sciences of Drexel University. Many thanks to Germantown Academy for site access and to Upper Gwynedd and Ambler wastewater treatment plants for discharge information. Thank you to the associate editor and 2 anonymous reviewers who helped strengthen this manuscript. All data used in this manuscript are publicly available from CUAHSI's HydroShare database: Ledford, S. H. (2020). Wissahickon Metabolism Data, HydroShare, http://www.hydroshare.org/resource/ce9e86dc4cbc4e71b6d330e32ea01df0

LITERATURE CITED

Alberts, J. M., J. J. Beaulieu, and I. Buffam. 2017. Watershed land use and seasonal variation constrain the influence of riparian canopy cover on stream ecosystem metabolism. Ecosystems 20:553–567.

Appling, A. P., and J. B. Heffernan. 2014. Nutrient limitation and physiology mediate the fine-scale (de)coupling of biogeochemical cycles. The American Naturalist 184:384–406..

Appling, A. P., R. O. Hall, C. B. Yackulic, and M. Arroita. 2018. Overcoming equifinality: Leveraging long time series for stream metabolism estimation. Journal of Geophysical Research: Biogeosciences 123:624–645.

Argerich, A., R. Haggerty, E. Martí, F. Sabater, and J. P. Zarnetske. 2011. Quantification of metabolically active transient storage (MATS) in two reaches with contrasting transient storage and ecosystem respiration. Journal of Geophysical Research 116, G03034.

Aristi, I., D. von Schiller, M. Arroita, D. Barceló, L. Ponsatí, M. J. García-Galán, S. Sabater, A. Elosegi, and V. Acuña. 2015. Mixed effects of effluents from a wastewater treatment plant on river ecosystem metabolism: Subsidy or stress? Freshwater Biology 60:1398–1410.

Beaulieu, J. J., C. P. Arango, D. A. Balz, and W. D. Shuster. 2013. Continuous monitoring reveals multiple controls on ecosystem metabolism in a suburban stream. Freshwater Biology 58(5):918–937.

Bernhardt, E. S., J. B. Heffernan, N. B. Grimm, E. H. Stanley, J. W. Harvey, M. Arroita, A. P. Appling, M. J. Cohen, W. H. McDowell, R. O. Hall, J. S. Read, B. J. Roberts, E. G. Stets, and C. B. Yackulic. 2018. The metabolic regimes of flowing waters. Limnology and Oceanography 63.

Blaen, P. J., M. J. Kurz, J. D. Drummond, J. L. A. Knapp, C. Mendoza-Lera, N. M. Schmadel, M. J. Klaar, A. Jäger, S. Folegot, J. Lee-Cullin, A. S. Ward, J. P. Zarnetsky, T. Datry, A. M. Milner, J. Lewandowski, D. M. Hannah, and S. Krause. 2018. Woody debris is related to reach-scale hotspots of lowland stream ecosystem respiration under baseflow conditions. Ecohydrology 11:1–9.

Burgin, A. J. and S. K. Hamilton. 2007. Have we overemphasized the role of denitrification in aquatic ecosystems? A review of nitrate removal pathways. Frontiers in Ecology and the Environment 5(2):89–96

Burgin, A. J., W. H. Yank, S. K. Hamilton, and W. L. Silver. 2011. Beyond carbon and nitrogen: How the microbial energy economy couples elemental cycles in diverse ecosystems. Frontiers in Ecology and the Environment 9:44–52.

Carey, R. O., and K. W. Migliaccio. 2009. Contribution of wastewater treatment plant effluents to nutrient dynamics in aquatic systems: A review. Environmental Management 44:205–217.

Center for Sustainable Communities. 2014. Wissahickon Creek Act 167 Plan, R. Fromuth (Ed). www.montcopa.org/2264/Wissahickon-Creek-Watershed-Act-167-Plan

Clapcott, J. E., R. G. Young, M. W. Neale, K. Doehring, and L. A. Barmuta. 2016. Land use affects temporal variation in stream metabolism. Freshwater Science 35:1164–1174.

Cirpka, O. A, N. M. Fienen, M. Hofer, E. Hoehn, A. Tessarini, R. Kipfer, and P. K. Kitanidis. 2007. Analyzing bank filtration by deconvoluting times series of electric conductivity. Ground Water 45:318–328.

Cohen, M. J., M. J. Kurz, J. B. Heffernan, J. B. Martin, R. L. Douglass, C. R. Foster, and R. G. Thomas. 2013. Diel phosphorus variation and the stoichiometry of ecosystem metabolism in a large spring-fed river. Ecological Monographs 83:155–176.

Covino, T. P., B. L. McGlynn, and R. A. McNamara. 2010. Tracer additions for spiraling curve characterization (TASCC): Quantifying stream nutrient uptake kinetics from ambient to saturation. Limnology and Oceanography: Methods 8:484–498.

De Lange, H. D., D. Morris, and C. Williamson. 2003. Solar ultraviolet photodegradation of DOC may stimulate freshwater food webs. Journal of Plankton Research 25:111–117.

Dodds, W. K. and E. B. Welch, 2000. Establishing nutrient criteria in streams. Journal of the North American Benthological Society 19:186–196.

Dodds, W. K., A. J. Lopez, W. B. Bowden, S. Gregory, N. B. Grimm, S. K. Hamilton, A. E. Hershey, E. Martí, W. H. McDowell, J. L. Meyer, D. Morrall, P. J. Mulholland, B. J. Peterson, J. L. Tank, H. M. Valett, J. R. Webster, and W. Wollheim. 2002. N uptake as a function of concentration in streams. Journal of the North American Benthological Society 21:206–220.

Ensign, S. H., and M. W. Doyle. 2006. Nutrient spiraling in streams and river networks. Journal of Geophysical Research 111.

Figueroa-Nieves, D., W. H. McDowell, J. D. Potter, and G. Martínez. 2016. Limited uptake of nutrient input from sewage effluent in a tropical landscape. Freshwater Science 35:12–24.

Gammons, C. H., J. N. Babcock, S. R. Parker, and S. R. Poulson. 2011. Diel cycling and stable isotopes of dissolved oxygen, dissolved inorganic carbon, and nitrogenous species in a stream receiving treated municipal sewage. Chemical Geology 283:44–55.

Gibson, C. A., and J. L. Meyer. 2007. Nutrient uptake in a large urban river. Journal of the American Water Resources Association 43:576–587.

González-Pinzón, R., R. Haggerty, and D. D. Myrold. 2012. Measuring aerobic respiration in stream ecosystems using the resazurin-resorufin system. Journal of Geophysical Research 117, G00N06.

González-Pinzón, R., R. Haggerty, and A. Argerich. 2014. Quantifying spatial differences in metabolism in headwater streams. Freshwater Science 33:798–811.

González-Pinzón, R., M. Peipoch, E. Marti, R. Haggerty, and J. H. Fleckenstein. 2016. Nighttime and daytime respiration in a headwater stream. Ecohydrology 9:93–100.

Gücker, B. and M. T. Pusch. 2006. Regulation of nutrient uptake in eutrophic lowland streams. Limnology and Oceanography 51:1443–1453.

Gücker, B., M. Braauns, and M. T. Pusch. 2006. Effects of wastewater treatment plant discharge on ecosystem structure and function of lowland streams. Journal of the North American Benthological Society 25:313–329.

Haggard, B. E., D. E. Storm, and E. H. Stanley. 2001. Effect of a point source input on stream nutrient retention. Journal of the American Water Resources Association 37:1291–1299.

Haggard, B. E., E. H. Stanley, and D. E. Storm. 2005. Nutrient retention in a point-source enriched stream. Journal of the North American Benthological Society 24:29–47.

Haggerty, R., A. Argerich, and E. Martí. 2008. Development of a “smart” tracer for the assessment of microbiological activity and sediment-water interaction in natural waters: The resazurin-resorufin system. Water Resources Research 44, W00D01.

Haggerty, R., E. Martí, A. Argerich, D. von Schiller, and N. B. Grimm. 2009. Resazurin as a "smart" tracer for quantifying metabolically active transient storage in stream ecosystems. Journal of Geophysical Research: Biogeosciences 114.

Haggerty, R., M. Ribot, G. A. Singer, E. Martí, A. Argerich, G. Agell, and T. J. Battin. 2014. Ecosystem respiration increases with biofilm growth and bed forms: Flume measurements with resazurin. Journal of Geophysical Research: Biogeosciences 119.

Hall, R. O., M. A. Baker, C. D. Arp, and B. J. Koch. 2009. Hydrologic control of nitrogen removal, storage, and export in a mountain stream. Limnology and Oceanography 54:2128–2142.

Hall , R. O., M. A. Baker, E. J. Rosi-Marshall, J. L. Tank, and J. D. Newbold. 2013. Solute-specific scaling of inorganic nitrogen and phosphorus uptake in streams. Biogeosciences 10:7323-7331

Hall, R. O. and E. R. Hotchkiss. 2017. Stream Metabolism. Pages 219-233. *in* Lamberti G. A. and F. R. Hauer (eds) Methods in Stream Ecology, Volume 2: Ecosystem Function. Academic Press, San Diego, CA.

Halvorson, H. M., E. E. Scott, S. A. Entrekin, M. A. Evans-White, and J. T. Scott. 2016. Light and dissolved phosphorus interactively affect microbial metabolism, stoichiometry and decomposition of leaf litter. Freshwater Biology 61:1006–1019.

Heffernan, J. B., and M. J. Cohen. 2010. Direct and indirect coupling of primary productivity and diel nitrate dynamics in a subtropical spring-fed river. Limnology and Oceanography 55:677–688.

Hensley, R. T., M. J. Cohen, and L. V. Korhnak. 2014. Inferring nitrogen removal in large rivers from high-resolution longitudinal profiling. Limnology and Oceanography 59:1152–1170.

Hensley, R., and M. J. Cohen. 2016. On the emergence of diel solute signals in flowing waters. Water Resources Research 52:759–772..

The Heritage Conservancy. 2012. Riparian Buffer Assessment. www.pasda.psu.edu/uci/DataSummary.aspx?dataset=36, accessed Feb. 13, 2019.

Hotchkiss, E. R., and R. O. Hall. 2014. High rates of daytime respiration in three streams: Use of $\delta^{18}O_{O2}$ and O_2 to model diel ecosystem metabolism. Limnology and Oceanography 59:798–810.

Kaplan, L. A., and T. L. Bott. 1982. Diel fluctuations of DOC generated by algae in a piedmont stream. Limnology and Oceanography 27:1091–1100.

Knapp, J. L. A., R. González-Pinzón, and R. Haggerty. 2018. The Resazurin-Resorufin System: Insights From a Decade of "Smart" Tracer Development for Hydrologic Applications. Water Resources Research 54:6877–6889.

Knapp, J. L. A., and O. A. Cirpka. 2018. A Critical Assessment of Relating Resazurin–Resorufin Experiments to Reach-Scale Metabolism in Lowland Streams. Journal of Geophysical Research: Biogeosciences 123:3538–3555.

Kurz, M. J., V. de Montety, J. B. Martin, M. J. Cohen, and C. R. Foster. 2013. Controls on diel metal cycles in a biologically productive carbonate-dominated river. Chemical Geology 358:61–74.

Kurz, M. J., J. D. Drummond, E. Martí, J. P. Zarnetske, J. Lee-Cullin, M. J. Klaar, S. Folegot, T. Keller, A. S. Ward, J. H. Fleckenstein, T. Datry, D. M. Hannah, and S. Krause. 2017.

Impacts of water level on metabolism and transient storage in vegetated lowland rivers: Insights from a mesocosm study. Journal of Geophysical Research: Biogeosciences 122:628–644.

Laursen, A. E., and S. P. Seitzinger. 2004. Diurnal patterns of denitrification, oxygen consumption and nitrous oxide production in rivers measured at the whole reach scale. Freshwater Biology 49:1448–1458.

Ledford, S. H., L. K. Lautz, P. G. Vidon, and J. C. Stella. 2017. Impact of seasonal changes in stream metabolism on nitrate concentration in an urban streama. Biogeochemistry 133:317–331.

Ledford, S. H., and L. Toran. 2020. Downstream evolution of wastewater treatment plant nutrient signals using high-temporal monitoring. Hydrological Processes 34:853–864.

Lemke, D., R. González-Pinzón, Z., Liao, T. Wöhling, K. Osenbrück, R. Haggerty, and O. A. Cirpka. 2014. Sorption and transformation of the reactive tracers resazurin and resorufin in natural river sediments. Hydrology and Earth System Sciences, 18:3151–3163.

Lorenzen J., L. H. Larsen, T. Kjaer, and N. P. Revsbech. (1998) Biosensor determination of the microscale distribution of nitrate, nitrate assimilation, nitrification, and denitrification in a diatom-inhabited freshwater sediment. Applied and Environmental Microbiology, 64:3264–3269.

Martí, E., J. Aumatell, L. Godé, M. Poch, and F. Sabater. 2004. Nutrient retention efficiency in streams receiving inputs from wastewater treatment plants. Journal of Environmental Quality 33:285–293.

McNicholl, B. P., J. W. McGrath, and J. P. Quinn. 2007. Development and application of a resazurin-based biomass activity test for activated sludge plant management, Water Research 41:127–133.

Mulholland, P. J., A. M. Helton, G. C. Poole, R. O. Hall, S. K. Hamilton, B. J. Peterson, J. L. Tank, L. R. Ashkenas, L. W. Cooper, C. N. Dahm, W. K. Dodds, S. E. G. Findlay, S. V. Gregory, N. B. Grimm, S. L. Johnson, W. H. McDowell, J. L Meyer, H. M. Valett, J. R. Webster, C. P. Arango, J. J. Beaulieu, M. J. Bernot, A. J. Burgin, C. L. Crenshaw, L. T. Johnson, B. R. Niederlehner, J. M. O'Brien, J. D. Potter, R. W. Sheibley, D. J. Sobota, and S. M. Thomas. 2008. Stream denitrification across biomes and its response to anthropogenic nitrate loading. Nature 452: 202–205.

Nielsen L.P., P. B. Christensen, N. P. Revsbech, J. and Sorensen. (1990) Denitrification and photosynthesis in stream sediment studied with microsensor and whole-core techniques. Limnology and Oceanography, 35:1135–1144.

Nimick D.A., C. H. Gammons, and S. R. Parker (2011), Diel biogeochemical processes and their effect on the aqueous chemistry of streams: A review. Chemical Geology 283, 3-17

O'Brien, J. M., I. Wilson, T. Orton, and F. Pognan. 2000. Investigation of the Alamar Blue (resazurin) fluorescent dye for the assessment of mammalian cell cytotoxicity. European Journal of Biochemistry 267:5421–5426.

Odum, H. T., 1956. Primary production in flowing waters. Limnology and Oceanography 1:102–117.

Owens, M., 1974. Measurements on non-isolated natural communities in running waters. In: Vollenweider, R.A. (Ed.), A Manual on Methods for Measuring Primary Production in Aquatic Environments. Blackwell Scientific Publications, pp. 111–119.

Perkins, D. M., G. Yvon-Durocher, B. O. L. Demars, J. Reiss, D. E. Pichler, N. Friberg, M. Trimmer, and G. Woodward. 2012. Consistent temperature dependence of respiration across ecosystems contrasting in thermal history. Global Change Biology 18:1300–1311.

Rahm, B. G., N. B. Hill, S. B. Shaw, and S. J. Riha. 2016. Nitrate dynamics in two streams impacted by wastewater treatment plant discharge: point sources or sinks? Journal of the American Water Resources Association 52:592–604.

Ramírez, A., C. M. Pringle, L. and Molina. 2003. Effects of stream phosphorus levels on microbial respiration. Freshwater Biology 48:88–97.

Reisinger, A. J., T. R. Doody, P. M. Groffman, S.S. Kaushal, and E. J. Rosi. 2019. Seeing the light: Urban stream restoration affects stream metabolism and nitrate uptake via changes in canopy cover. Ecological Applications, e01941.

Ribot, M., J. Cochero, T. N. Vaessen, S. Bernal, E. Bastias, E. Gacia, A. Sorolla, F. Sabater, and E. Martí. 2019. Leachates from helophyte leaf-litter enhance nitrogen removal from wastewater treatment plant effluents. Environmental Science and Technology 53:7613–7620.

Schmadel, N. M., A. S. Ward, M. J. Kurz, J. H. Fleckenstein, J. P. Zarnetske, D. M. Hannah, T. Blume, M. Vieweg, P. J. Blaen, C. Schmidt, J. L. A. Knapp, M. J. Klaar, R. Romeijn, T. Datry, T. Keller, S. Folegot, A. I. Marruedo Arricibita, and S. Krause. 2016. Stream solute tracer timescales changing with discharge and reach length confound process interpretation. Water Resources Research 52:3227–3245.

Siejak, P. and D. Frackowiak (2005) Spectral properties of fluorescein molecules in water with the addition of a colloidal suspension of silver. The Journal of Physical Chemistry B 109 :14382–14386.

Sinsabaugh, R. L.1997. Large-scale trends for stream benthic respiration. Journal of the North American Benthological Society 16:119–122.

Smith, V. H., 2003. Eutrophication of freshwater and coastal marine ecosystems a global problem. Environmental Science and Pollution Research, 10:126–139.

Stream Solute Workshop. 1990. Concepts and methods for assessing solute dynamics in stream ecosystems. Journal of the North American Benthological Society 9:95–119.

Strotmann, U. J., B. Butz, and W. R. Bias. 1993. A dehydrogenase assay with resazurin-practical performance as a monitoring-system and pH-dependent toxicity of phenolic-compounds. Ecotoxicology and Environmental Safety 25:79–89.

Tank, J. L., E. J. Rosi-Marshall, M. A. Baker, and R. O. Hall, Jr. 2008. Are rivers just big streams? A pulse method to quantify nitrogen demand in a large river. Ecology 89:2935–2945.

Tobias, C. R., J. K. Böhlke, and J. W. Harvey. 2007. The oxygen-18 isotope approach for measuring aquatic metabolism in high-productivity waters. Limnology and Oceanography 52:1439–1453.

United States Environmental Protection Agency. 2003. Nutrient and siltation TMDL development for Wissahickon Creek, Pennsylvania. Final Report, October 2003.

van Meter, K. J., P. van Cappellen, and N. B. Basu. 2018. Legacy nitrogen may prevent achievement of water quality goals in the Gulf of Mexico. Science 360:427–430.

Ward, A. S., N. M. Schmadel, S. M. Wondzell, C. Harman, M. N. Gooseff, and K. Singha. 2016. Hydrogeomorphic controls on hyporheic and riparian transport in two headwater mountain streams during base flow recession. Water Resources Research 52:1479–1497.

Ward, A. S., M. J. Kurz, N. M. Schmadel, J. L. A. Knapp, P. J. Blaen, C. J. Harman, J. D. Drummond, D. M. Hannah, S. Krause, A. Li, E. Martí, A. Milner, M. Miller, K. Neil, S. Plont, A. I. Packman, N. I. Wisnoski, S. M. Wondzell, and J. P. Zarnetsky. 2019. Solute transport and transformation in an intermittent, headwater mountain stream with diurnal discharge fluctuations. Water 11:2208.

Wassenaar, L. I., J. J. Venkiteswaran, S. L. Schiff, and G. Koehler. 2010. Aquatic community metabolism response to municipal effluent inputs in rivers quantified using diel $\delta^{18}O$ values of dissolved oxygen. Canadian Journal of Fisheries and Aquatic Science 67:1232–1246.

FIGURES

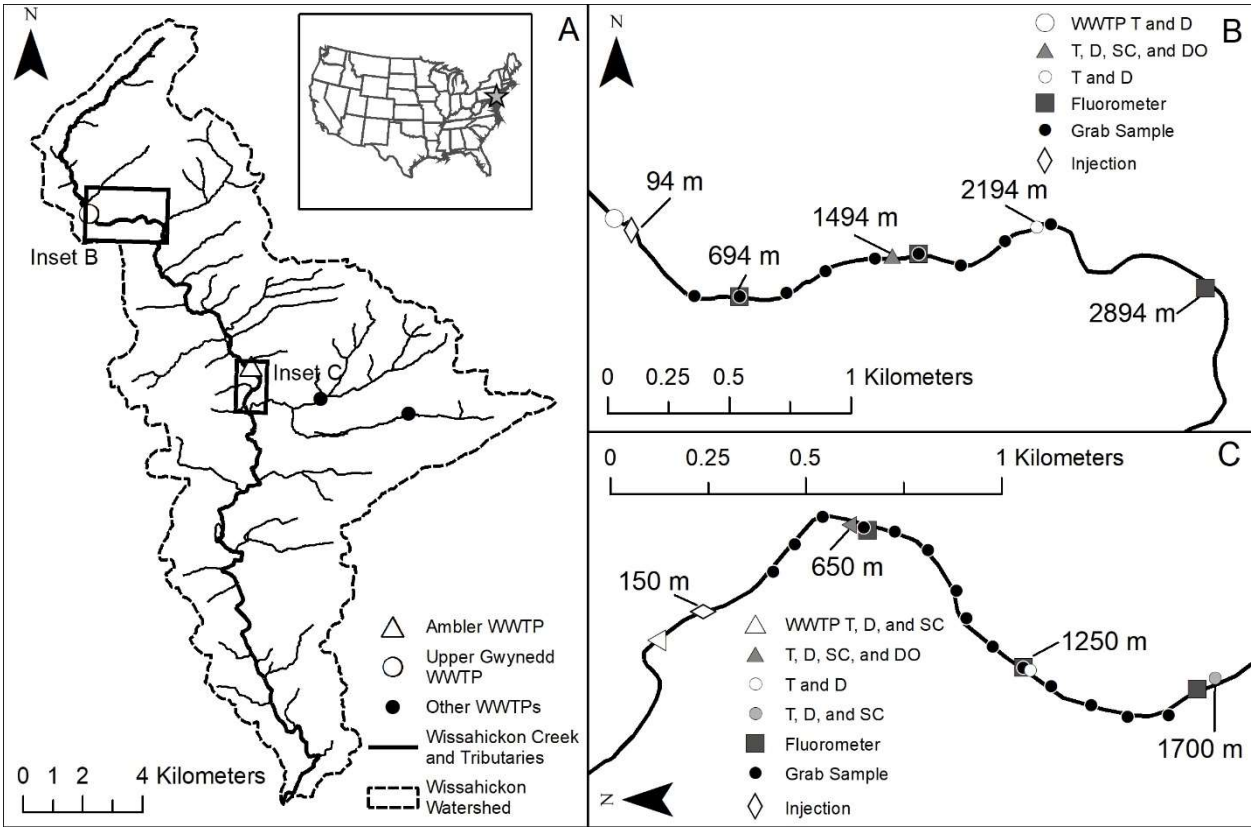

Fig. 1. Wissahickon Creek watershed, located in Montgomery and Philadelphia counties, Pennsylvania, USA, is a suburban-urban watershed (A). Reach 1 is located downstream of the Upper Gwynedd wastewater treatment plant (WWTP) in the headwaters of the stream (B). Reach 2 is located ~10 km further downstream, downstream of the Ambler WWTP (C). Maps show where temperature (T), depth (D), specific conductivity (SC) and dissolved oxygen (DO) were measured. The inset map indicates where this watershed is located in the contiguous United States.

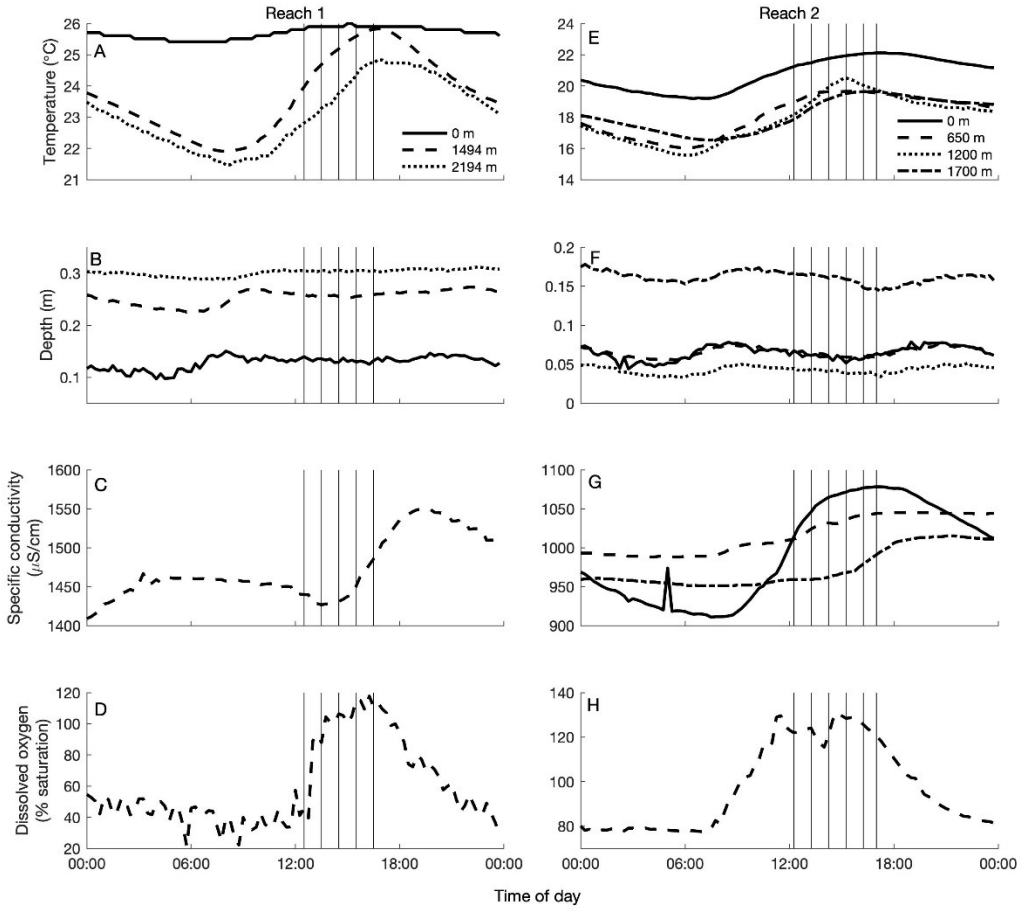

Fig. 2. Logger data from different longitudinal locations within each reach. The left column is reach 1, showing measurements of temperature (A), depth (B), specific conductivity (C), and dissolved oxygen (D) at the waste water treatment plant (WWTP; 0 m), 1400 m downstream of the plant, and 2100 m downstream of the plant (not all parameters were measured at each site). All measurements at reach 1 were taken on 26 September 2017. The right column is reach 2, showing measurements of temperature (E), depth (F), specific conductivity (G), and dissolved oxygen (H) at the WWTP (0 m) and 600, 1200, and 1700 m downstream of the plant (not all parameters were measured at all sites). All measurements at reach 2 were taken on 12 September 2017. Vertical lines in all panels indicate timing of grab sample collection.

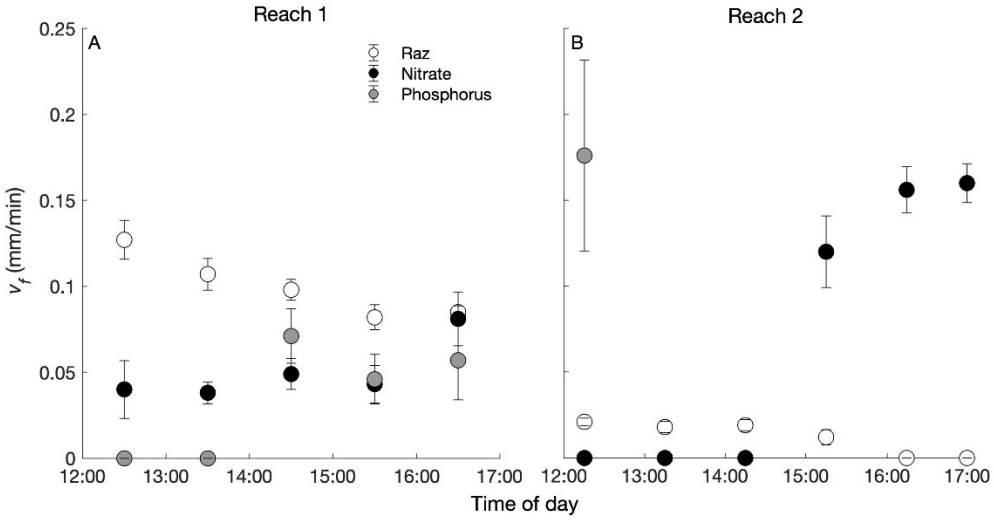

Fig. 3. Uptake rates over the afternoon at reach 1 (A) and reach 2 (B) for Raz, nitrate, and phosphorus. Error bars represent the standard error of *k* multiplied by average depth. At reach 2, TDP only had 1 detectible uptake period, and the rest were 0.

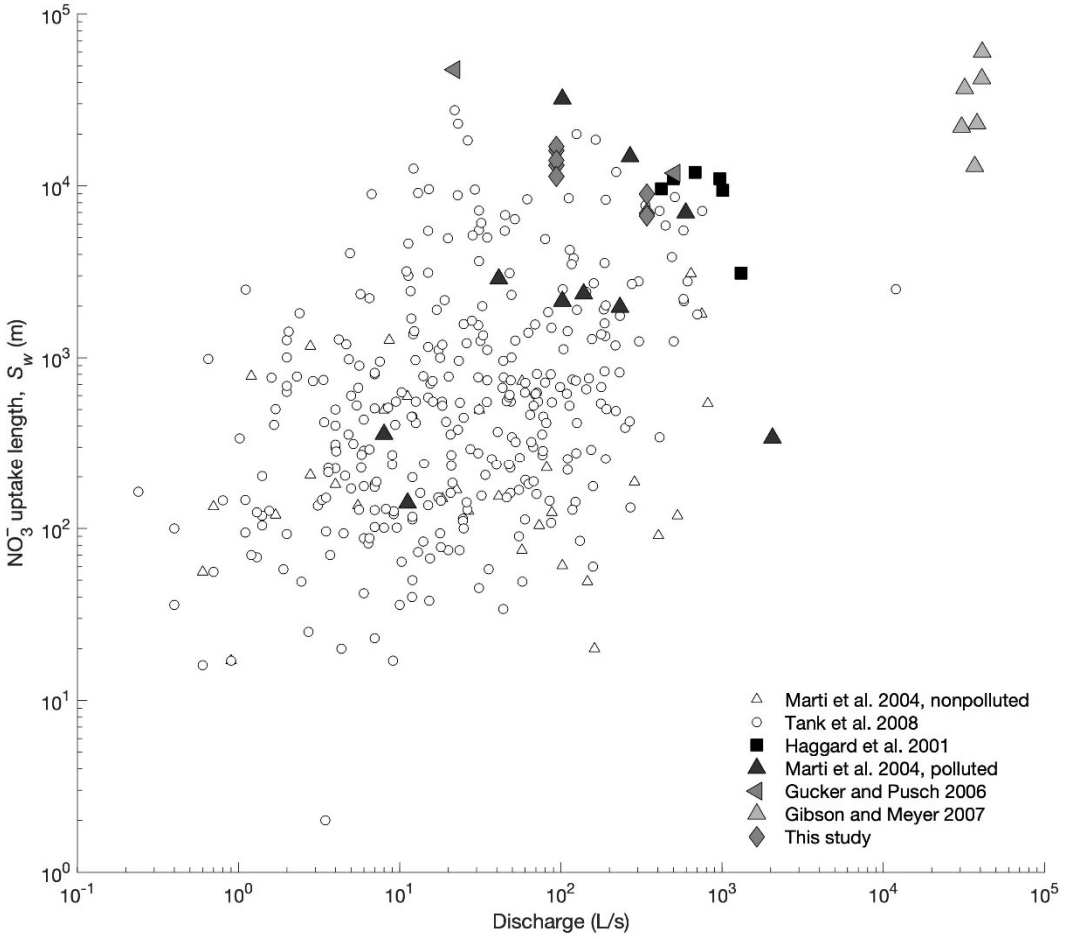

Fig. 4. Estimated nitrate uptake length in both study reaches relative to those reported for other streams that received waste water treatment plant (WWTP) effluent (filled points) and did not receive WWTP effluent (open points). Data from Haggard et al. 2001, Martí et al. 2004, Gücker and Pusch 2006, Gibson and Meyer 2007, and Tank et al. 2008.

Table 1. Major structural and transport parameters compared between sites. Bolded values indicate higher relative values between reaches. Ranges that are temporal are indicated with ^{T} and ranges that represent spatial change are indicated with ^{S}.

Parameter	Reach 1	Reach 2
Discharge (m^3/s) (± SE)	0.09 (±8%)	**0.34** (±7.2%)
Velocity (m/s)	0.06	**0.12**
Specific discharge (m^2/s)	0.011	**0.019**
Mean depth (m)	0.22 (0.12–0.28)^{S}	0.21 (0.10–0.31)^{S}
Mean width (m)	8.4 (6.6–11.6)^{S}	**19.0 (12.1–26.3)**^{S}
Reach μ_2 (h^2)	**0.38**	0.17
Reach μ_3 (h^3)	**0.37**	0.08
Reach CV	0.20	0.22
Reach skewness, ɣ	**1.61**	1.13
D_{app} (x10^4 m^2/h)	**3.8**	1.5
pH	7.73–8.55^{T}	8.44–8.66^{T}
Canopy coverage (average % open)	35.3% (23.9–48.9%)^{S}	44.8% (35.1–67.6%)^{S}

Table 2. Major metabolic parameters compared between sites. Bolded values indicate higher values between reaches, with p-values <0.05 using ANOVA. Sampling intervals with insignificant uptake or release are not reported but indicated with < for uptake rates and velocities or > for uptake lengths. Up or down arrows indicate increasing or decreasing temporal trends during the afternoon study period with *p*-values reported. No arrow means there was no temporal trend in that variable over the afternoon. All ranges are temporal.

Parameters	Reach 1	Reach 2
NO_3^- (mg N/L)	**18.2–19.0**	10.2–11.1 (↑ $p = 0.03$)
Average NO_3^- flux (g/s)	1.7	**3.9**
TDP (mg/L)	**0.37–0.47** (↑ $p = 0.002$)	0.27–0.36 (↑ $p = 0.04$)
Average TDP flux (mg/s)	37	**120**
GPP (g O_2 m^{-2} d^{-1})	2.7 (0.9 – 4.9)	**7.0 (4.3–10.8)**
ER (g O_2 m^{-2} d^{-1})	–7.4 (–5.6– –8.9)	**–10.1 (–7.2– –13.3)**
# significant Raz transformation	5 (of 5)	4 (of 6)
Raz $k_{t,ad}$ (x10^{-4} min^{-1})	**3.74–5.77** (↓ $p = 0.02$)	<0.57–0.98 (↓ $p = 0.007$)
Raz V_f (mm/min)	**0.082–0.127** (↓ $p = 0.02$)	<0.012–0.021 (↓ $p = 0.007$)
# significant N uptake	5 (of 5)	3 (of 6)
NO_3^- S_w (km)	**7.9–16.9**	6.7–>9.0
NO_3^- V_f (mm/min)	0.038–0.081	**<0.120–0.160** (↑ $p = 0.009$)
NO_3^- U (mg N m^{-2} d^{-1})	988–2235	**<1831–2554** (↑ $p = 0.008$)
# significant TDP uptake	3 (of 5)	1 (of 6)
TDP S_w (km)	**9.0–>14.1**	6.1–>6.1

TDP V_f (mm/min)	<0.046–0.071	**<0.176–0.176**
TDP U (mg m^{-2} d^{-1})	<28–42	**<80–80**

Supplemental Information for

Contrasting Raz-Rru stream metabolism and nutrient uptake downstream of urban wastewater effluent sites

Sarah H. Ledford*, Marie Kurz, and Laura Toran

*Corresponding author: sledford@gsu.edu

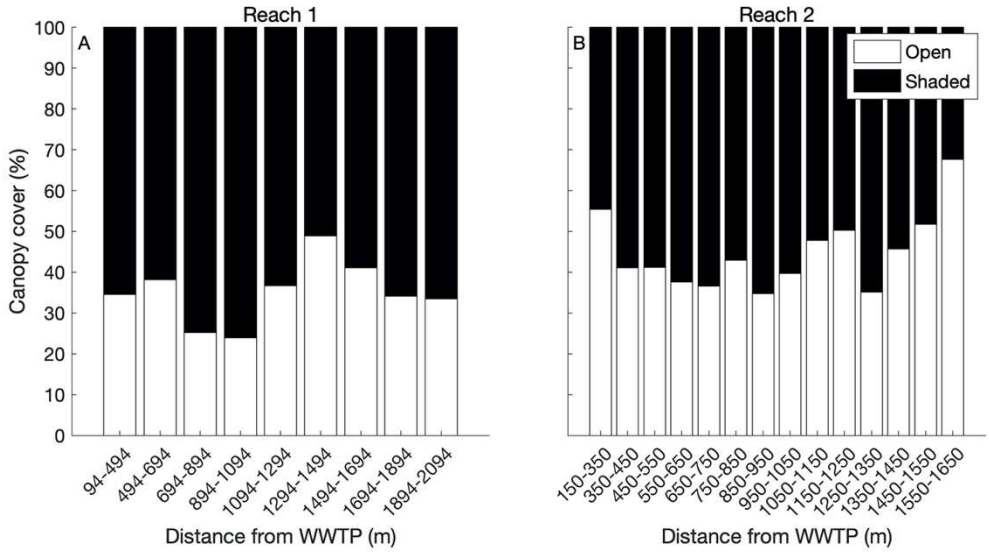

Fig. S1. Canopy cover with distance over reach 1 (A) and reach 2 (B) as measured from aerial imagery. Percentage of open channel is represented by white bars, and percentage of covered channel is represented by black bars.

Fig.

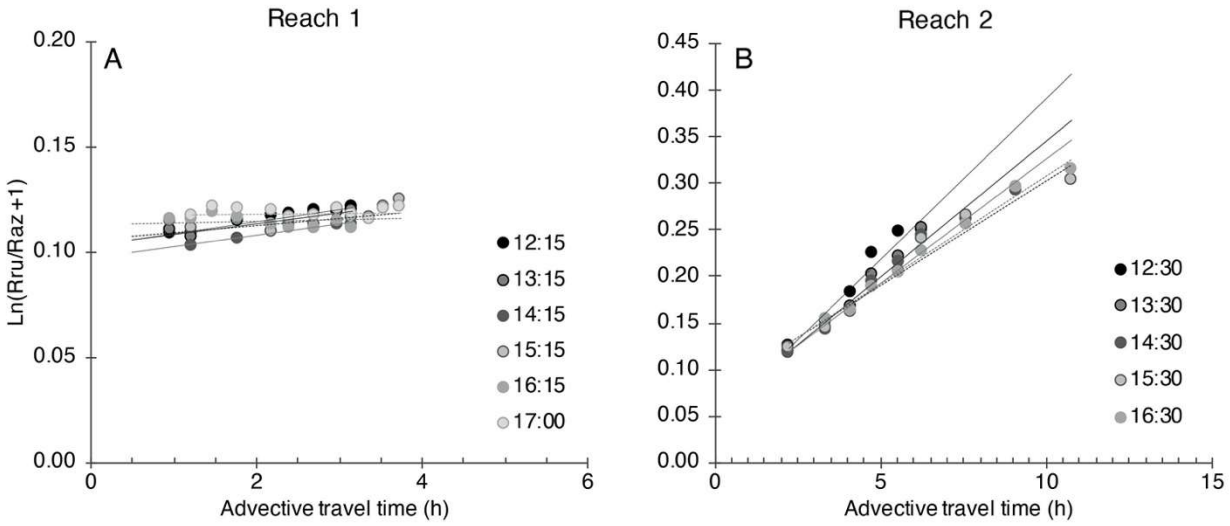

S2. Plots of longitudinal tracer concentrations based on grab samples collected during

the tracer plateau. Slopes used to calculate Raz $k_{t,ad}$ and V_f.

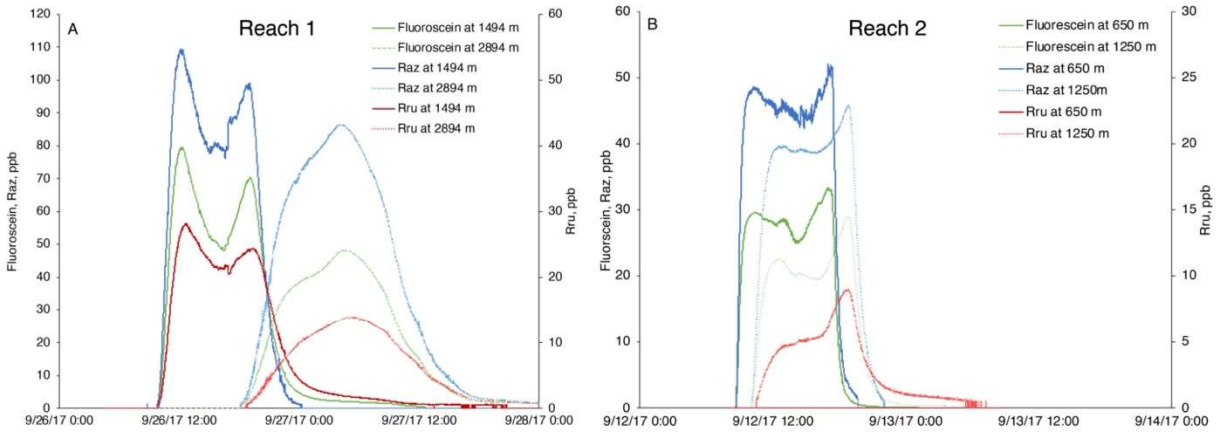

Fig. S3. Breakthrough curves at reach 1 (A) and reach 2 (B).

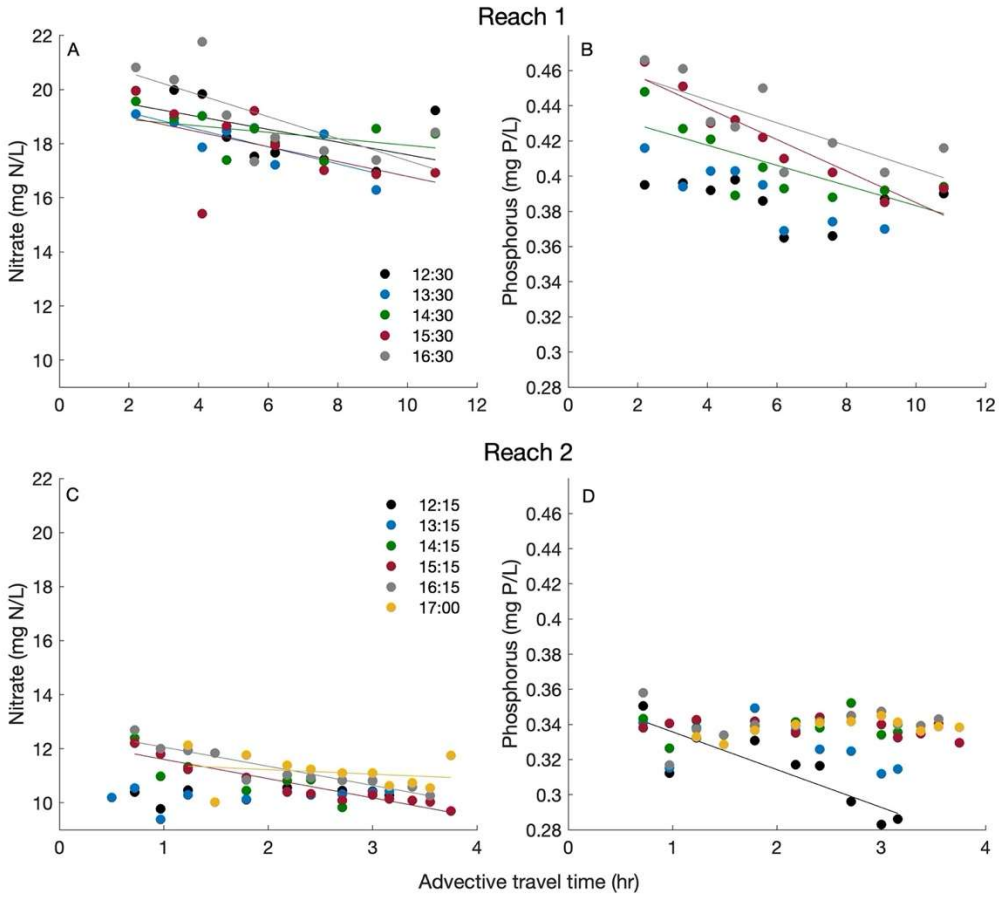

Fig. S4. Longitudinal nitrate (A and C) and total dissolved phosphorus (B and D) patterns along the upper (A and B) and lower (C and D) reaches. Time periods with regression lines show periods where normalized nutrients declined with distance.

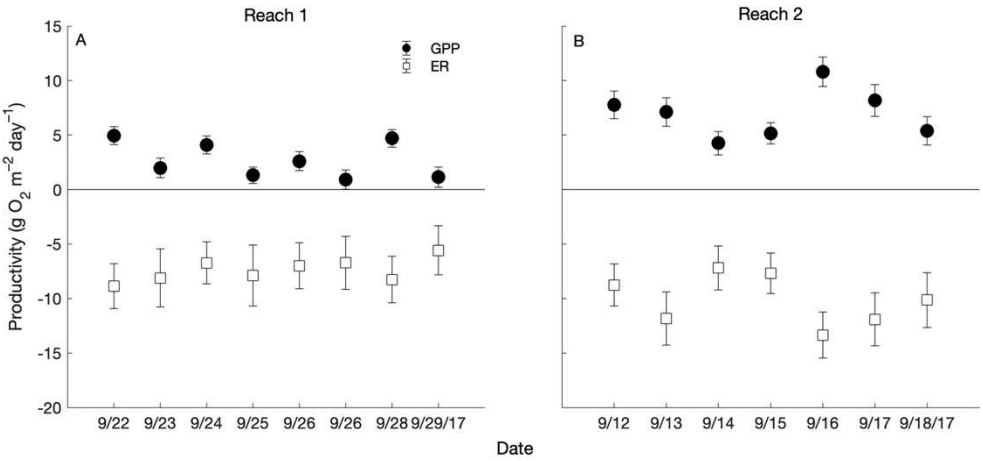

Fig. S5. Daily gross primary productivity (GPP) and ecosystem respiration (ER) results for the 7 to 8 days of data used at each site.

Table S1. ANOVA regression results for each uptake regression. The first value reported is the *p*-value and the second is *n*. Values in bold indicate *p*-values <0.06. '*No retention*' indicates there was a positive slope at that time period, indicating nutrient release.

Site	Time	N	P	Raz-Rru
Reach 1	12:30	**0.055; 8**	*No retention*	**0.0004; 6**
Reach 1	13:30	**0.002; 7**	*0.38; 8*	**8.9E-5; 7**
Reach 1	14:30	**0.003; 7**	**0.006; 7**	**3.6E-6; 8**
Reach 1	15:30	**0.01; 9**	**0.02; 8**	**3.0E-5; 8**
Reach 1	16:30	**0.003; 7**	**0.057; 7**	**4.2E-7; 8**
Reach 2	12:15	*No retention*	**0.016; 9**	**8.3E-5; 8**

Reach 2	13:15	*No retention*	*0.13; 8*	**0.001; 8**
Reach 2	14:15	*0.29; 9*	*No retention*	**0.002; 7**
Reach 2	15:15	**0.0002; 12**	*No retention*	**0.03; 10**
Reach 2	16:15	**1.7E-7; 13**	*No retention*	*0.57; 12*
Reach 2	17:00	**6.1E-7; 10**	*0.77; 10*	*0.86; 11*